npdγ H/^{3}He Ion Chamber Technical Note

Christopher S. Blessinger

November 16, 2000

The last beam line element of the npdγ experiment is the H/^{3}He ion chamber used to monitor the transmitted neutron beam (figure 1). This device can be used to measure the neutron energy spectrum in current mode on a pulse by pulse basis. This device can be used in the experiment for a number of purposes, including (1) a veto for neutron pulse intensities that are significantly outside the normal intensity range, (2) a transmission detector for any neutron polarization analyzer that might be inserted behind the liquid hydron target, (3) an indirect measurement of the ortho/para ratio in the liquid hydrogen target, (4) a check on the gamma detector signal intensity, whose integral should be measuring most of the neutrons that are captured in the target, and (5) a measurement of the time of flight energy scale of the neutrons.

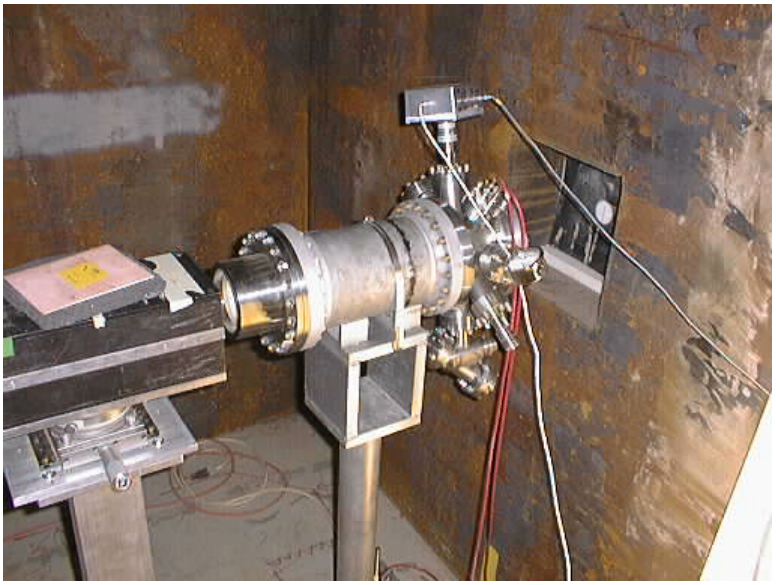

Figure 1: back monitor, beam path runs from left to right

The following requirements led to the choice of a ^{3}He-based ion chamber: (1) operation in current mode using the same electronics as the gamma detectors, (2) a well-understood detector efficiency as a function of neutron energy

over a large energy range(meV to .1 eV), (3) low sensitivity to gammas, (4) and no gamma ray production in the device itself.

The neutron beam is detected through the reaction:

$$n + {}^3\mathrm{He} \rightarrow {}^3\mathrm{H} + p + 0.78\mathrm{MeV}$$

The kinetic energies of the triton and proton ionize the gas as they slow down. These ions are then accelerated by an electric potential to electrodes and the charge on the electrodes is measured. There are several concerns which determine the gas mixture and the geometry of the device. All of the neutrons over a wide range(meV to eV) of energies need to be captured. This sets a lower limit on the total amount of ^{3}He intercepting the beam. The maximum density of ^{3}He is set by acceptable size of the the wall effect on the front vacuum window. The range of the proton and triton within the chosen gas mixture needs to be small compared to the reaction volume or much of the energy will be lost in wall effects as the proton and triton collide with the electrodes. The mobility of the ions needs to be large so that all of the those produced create current in the electrodes in a timely manner. Higher electric potentials will accelerate ions faster but will limit the gas mixture to one with a high breakdown voltage.

The gas mix was chosen to be 0.5 atm ^{3}He and 3 atm H_2. Hydrogen has low Z so the γ sensitivity is low and the mobility of its ions within itself is 13.0 $\frac{cm^2}{sec*V*atm}$. 3 atm of Hydrogen still stops the proton and triton within a few cm, while it has a breakdown voltage of $62\frac{kV}{cm}$.

The neutron absorption cross-section on ^3He is so high that the large scattering cross-section on H does not significantly effect the operation of the device.

The ion chamber consists of ten 3 inch diameter independent longitudinal segments. Each segment includes a collection electrode sandwiched between high voltage electrodes and guard rings. A side view of the assembled monitor is shown in figure 2. Expanded views of the separate plates are shown in figures 3 through 5.

The collection electrodes are thin(about .030"thick) 3" diameter Al sheets supported by insulating ceramic rings. The electrical connections are made mechanically by crimping wires under the screws which secure the electrodes to the rings.

The high voltage electrodes are Al sheets identical to the collection electrodes. The HV electrodes are clamped to the copper rings. Each copper ring is brazed to a copper wire which makes the electrical connection to the high voltage input.

The half voltage guard rings are the same as the full voltage plate except they lack the electrode. Located halfway between the HV plates and the collection plates and holding half the voltage of a HV plate, they serve to straighten the field.

This geometry of alternating collection and HV plates causes the voltage along the axis of the chamber to form a sawtooth potential that varies from 0V to the high voltage setting(usually 3kV).

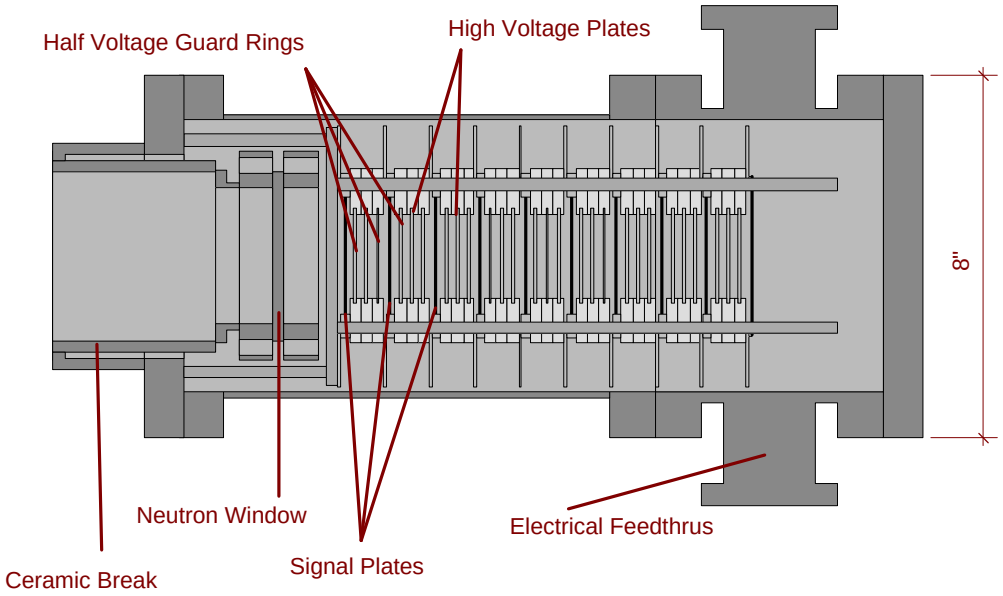

Figure 2: backmonitor assembly

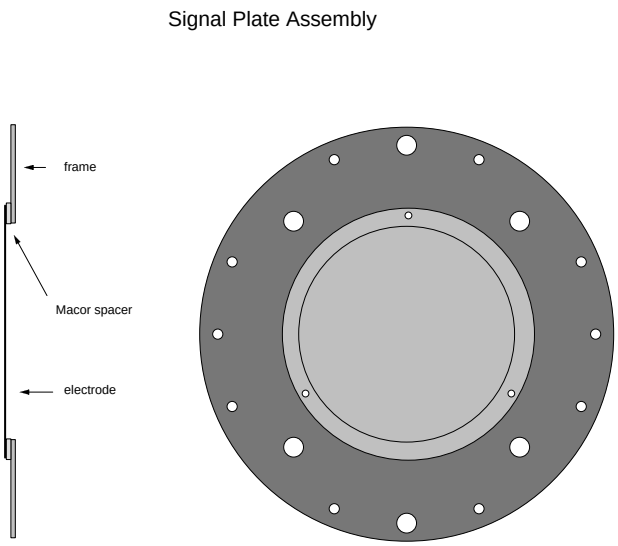

Figure 3: collection plate

The electrodes are separated by ceramic spacers suspended on rods and the whole assembly is enclosed in an Al UHV chamber to protect the purity of the gas mixture. The front window of the UHV chamber is itself a high voltage plate in order to utilize the ions produced in the front of the chamber. The rear of the chamber has UHV connections for the signal outputs, the high voltage inputs (the full and half voltages for the plates and guard rings are fed in separately), a pressure gauge, and the pumpout port.

Due to the mechanical difficulty of making the high vacuum/high voltage window the space between the front window and the first collection plate does not conform to the other plate spacings, nor does it have a guard ring. Similiarly, mechanical constraints on the electrical connections prevented placing a high voltage plate and half voltage guard ring after the last collection plate. These "end effects" make it difficult to include plates one and ten in comparisons between the performance of the plates.

The thin Al of the electrodes allows the neutrons to pass through mostly unattentuated, while the high cross section of the ^{3}He stops the neutrons between the plates. The resulting ions are accelerated by the sawtooth electric potential of the high voltage plates to the nearest collection plate. These ions produce current signals which are then the inputs of ten I$\rightarrow$V ampli-

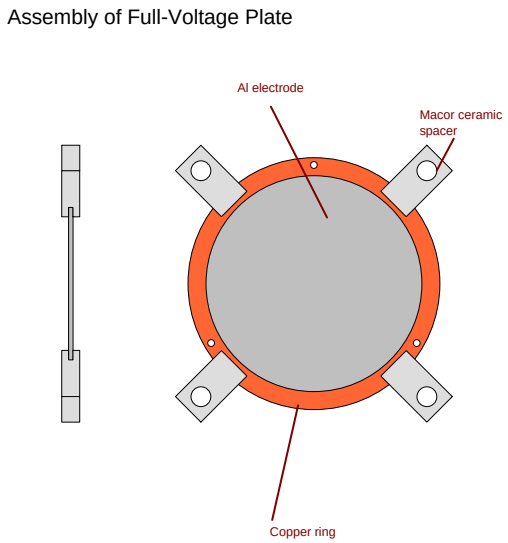

Figure 4: high voltage electrode

fiers (figure 6). The collection plate signals exit the chamber through two ports(plates 1 to 5 through one, plates 6 through 10 through the other). The amplifiers are built on circuit boards that are enclosed in metal housings mounted directly to the electrical feedthrough ports of the chamber. The voltage signals from thes amplifiers are then convenient to read by ADC.

Figure 7 shows the signal from all ten of the ion chamber plates. The feedback resistor on the preamps for this data was 100MΩ. The largest signal is from the front plate and the signal size shrinks with each following plate.

In order to relate time of flight of the neutrons to the energy of the neutrons, it is necessary to know the position of the ion chamber relative to the moderator. By increasing the sampling rate in the DAQ, a datarun (run00001919) was taken with the time resolution increased by a factor of ten (to .04mS per sample) so that the Bragg edges in the spectrum could be measured accurately. Figure 8 shows the data taken in this run. The notches centered at 25.76ms and 22.32ms are respectively the 200 and 111 Al Bragg edges generated by the vacuum and spin flipper windows in the beam. Time of flight is porportional to wavelength of the neutron (λ is porportional to

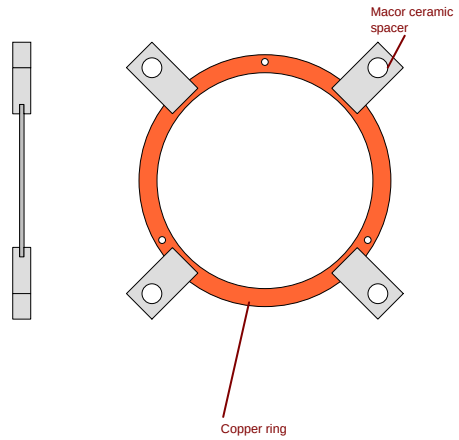

Figure 5: half voltage guard ring

$\frac{1}{v}$ which is in turn porportional to $\frac{t}{L}$ and L,the length of the flight path, is fixed). So the time of flight of these two edges should be separated by a factor equal to the plane separation in the crystal or $\frac{\sqrt{3}}{2}$; which they are (within the .04ms time resolution). The length of the flight path can be calculated by the following method:

$$2d\sin(\theta) = n\lambda$$

$$\lambda = \frac{h}{p} = \frac{ht}{mL}$$

$$h = 4.14 * 10^{-15}\text{eVs}$$

$$m = 939.6\frac{\text{MeV}}{c^2}$$

$$\theta = \frac{\pi}{2}; d = .46\text{nm}; n = 2$$

$$t = 25.76 \pm .04\text{ms}$$

Therefore,

$$L = 22.21 \pm .05\text{m}$$

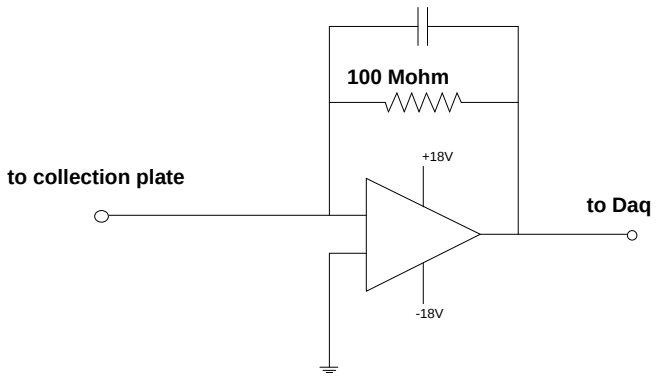

Figure 6: preamp

To show that the detector signal is due to neutron capture, we performed two experiments.

First, we placed a 2.4mm thick sheet of ^{6}Li plastic (17.1% Li by weight) intersecting the beam in order to stop the neutrons without creating gammas. Figure 9 shows the response of the front plate to the shielded beam in red; the blue trace is an example of the unattenuated neutron spectrum for comparison.

The peak at low time of flight is due to the fast neutrons penetrating the ^{6}Li absorber. The black line which overlaps the red line, is a calculation of the ^{6}Li absorption effect using the following method:

$$\frac{\text{Transmitted}}{\text{Incident}} = e^{-nl\sigma_a}$$

where

$$n = 3.022 * 10^{22} atom/cc \leftarrow {}^6\text{Li number density}$$

$$l = 2.4mm \leftarrow \text{absorber thickness}$$

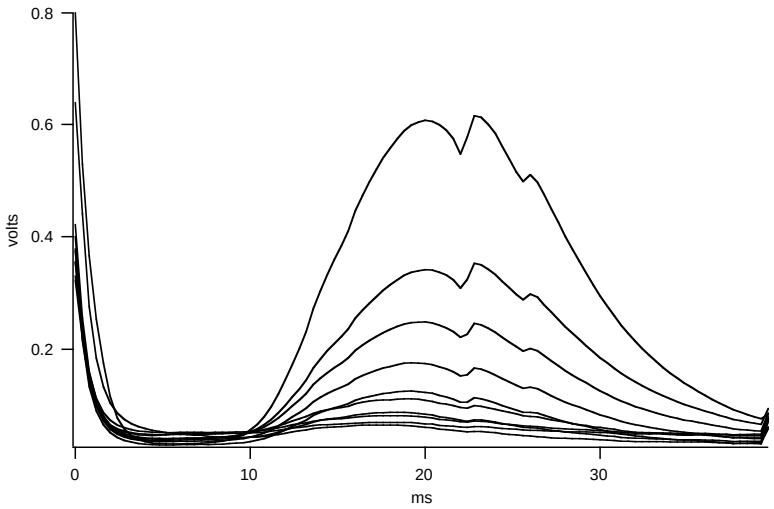

Figure 7: ten plates

$$\sigma_a = \sigma_o \frac{v_o}{v}$$

$$\sigma_o = 938b \leftarrow \text{n } {}^6\text{Li absorption cross section}$$

$$v_o = 2200 \frac{m}{s}$$

$$v = \frac{L}{t} = \frac{22.21m}{t}$$

Secondly, we attempted to measure the gamma sensitivity of the chamber by placing a 1 cm thick B_4C absorber, essentially converting every neutron in the beam into a 0.5 MeV gamma ray. However, we found that the response of the chamber to these gammas was so low that it was buried in the electronic noise.

It is also important to know if all of the ions produced are captured in the electrodes. In other words, that the chamber is operating in the linear region. As the bias is increased more and more ions reach the collection plates until all the ions produced are collected. At this point, more bias won't increase the signal. If too much bias is applied arcing will occur. Figure 10 shows the maximum signal voltage plotted against the bias. With our high voltage supply we were unable to overbias the chamber. We generally operated the chamber at 3kV which is far into the flat region.

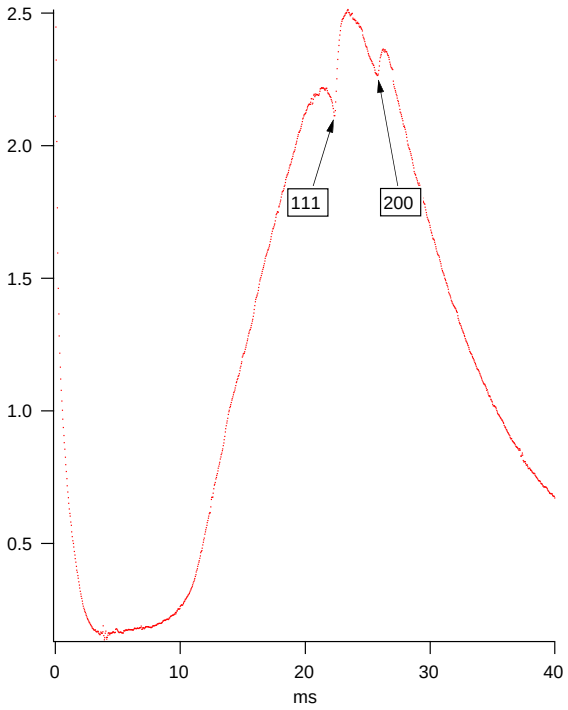

Figure 8: Al Bragg edges

Finally it is important to know how the spectrum changes as the beam passes through the chamber. Not only is it reduced in magnitude, but the shape changes as well. This is because of the $\frac{1}{v}$ cross section of the ^3He. Only a small fraction of the very fast neutrons are captured in each plate. The number of fast neutrons in the beam is only slightly changed as the beam progresses, which means that the small fraction on changes slightly. On the other hand, the slow neutrons are heavily attenuated in each plate which leaves a smaller and smaller beam for each succeeding plate to measure. The calculation for the change in the beam is similiar to the preceding ^6Li calculation and is shown below:

$$s_x(t) = e^{-nl\sigma_a} s_0(t)$$

where

$s_x(t)$ is the spectrum of plate x

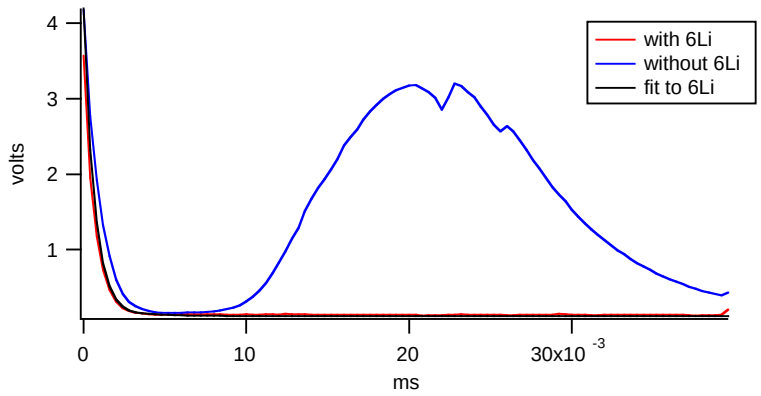

Figure 9: signal from the first plate when a ^{6}Li absorber intersects the beam

$$n = 1.34 * 10^{19} atom/cc \leftarrow {}^3\text{He number density}$$

$$l = 2.5cm$$

$$\sigma_a = \sigma_o \frac{v_o}{v}$$

$$\sigma_o = 5327b \leftarrow {}^3\text{He cross section}$$

$$v_o = 2200 \frac{m}{s}$$

$$v = \frac{L}{t} = \frac{22.21m}{t}$$

Figure 11 shows the comparison between the measured signals and the calculated estimate. These calculations have been done for plates number two through five(We started from plate two because of the geometric complexity of plate one). The black crosses are data; the red lines are calculation. Everything is normalized to plate two.

In general, noise in the ion chamber signals was caused by one of three sources: microphonic noise, pre-amp noise, or EM pick-up. Of the three, the pick-up was by far the worst because many electrical signals, particularly the RFSF, were correlated with the beam T_0 and were not averaged out by the pulse summing of the DAQ.

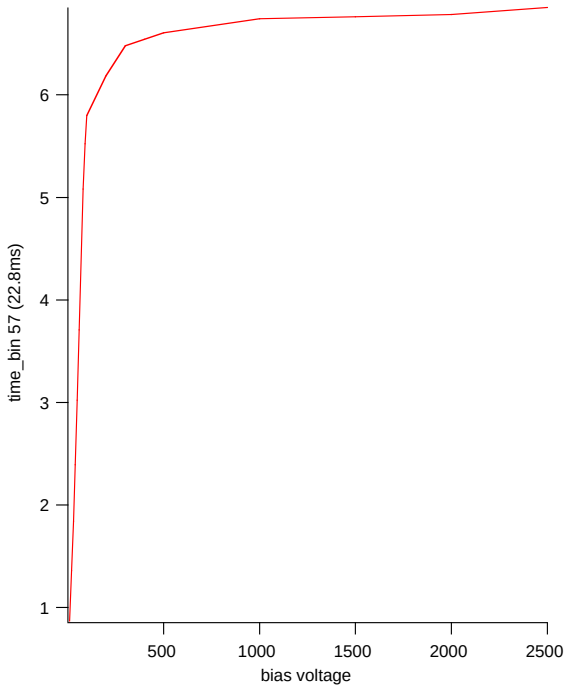

Figure 10: peak signal in Plate 1

The best assessment of the linearity of the ion chamber is actually the analysis of the ^{3}He transmission data in "NPDGamma Polarized ^{3}He Spin Filter Technical Note" which was taken using this device. The ^{3}He transmission varies over a large range and differs from theory by less than 1%.

From "Absolute Flux Measurement-Preliminary Summary", it was shown that the neutron beam intensity at its peak is $1.12*10^6 \frac{neutrons}{pulse\ second}$. This compares to plate one's voltage of about 0.6V and plate ten's voltageof about 0.06V. The feedback resistor on the preamp was 100MΩ, so one 1uA of input yieds 1V of output. Therefore, the sensitivity of the ion chamber is on the order of 50 to 500fC per neutron depending on the plate and the neutron energy or 50 to 500nV per neutron/s

From these results, we conclude the ion chamber meets the design goals.

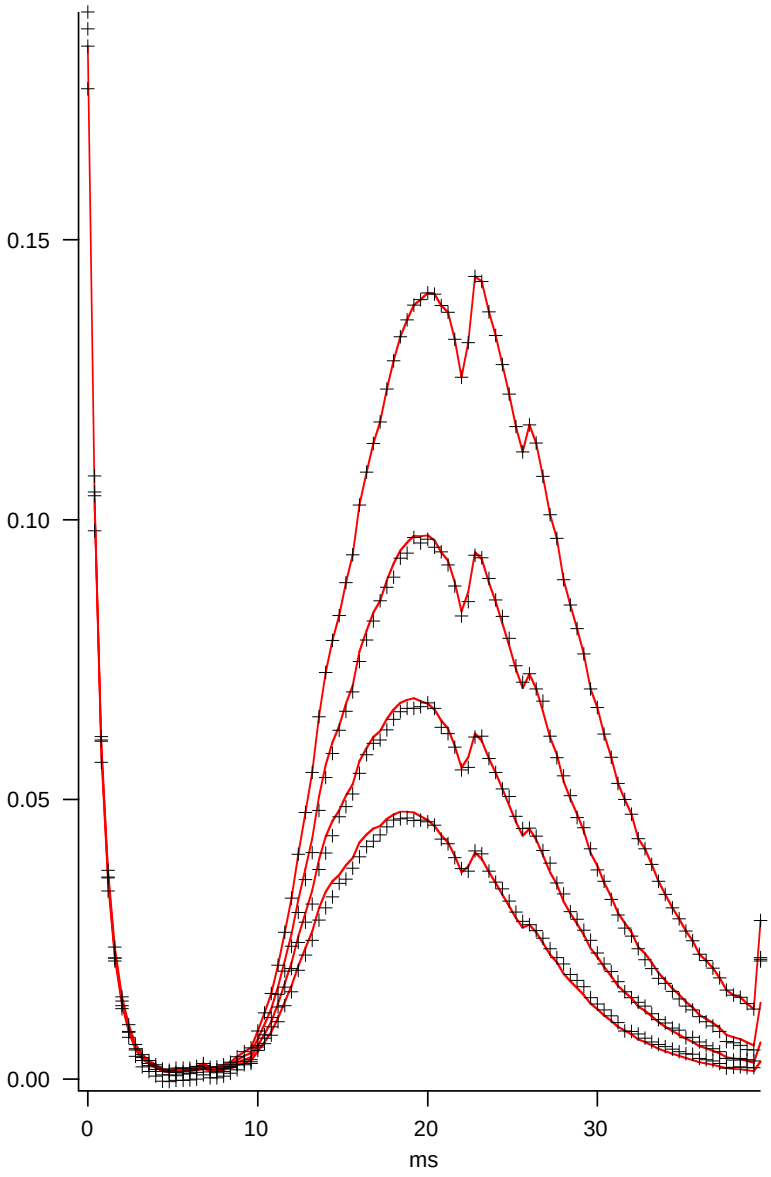

Figure 11: evolution of the spectrum from plates 2 to 5